Shunt Active Power Filter Control using Adaptive Algorithms NLMS and QR-RLS

Radek Martinek, Jaroslav Rzidky, Rene Jaros, Lukas Danys, Jan Baros, and Petr Bilik

Department of Cybernetics and Biomedical Engineering, Faculty of Electrical Engineering and Computer Science, VSB–Technical University of Ostrava, Czech Republic.

Email: radek.martinek@vsb.cz; jaroslav.rzidky@vsb.cz; rene.jaros@vsb.cz; lukas.danys@vsb.cz; jan.baros@vsb.cz; petr.bilik@vsb.cz

***Abstract* - This paper describes experimental verification of progressive control strategies for shunt active power filters (SAPF) in common single-phase systems. Normalized least mean squares (NLMS) and QR decomposition-based least squares (QR-RLS) were used as SAPF control adaptive algorithms. The functionality was verified on real data using a measuring system based on virtual instruments (modules NI 9225 and NI 9227 were inserted into the cDAQ 9185 chassis). Commonly household devices (TV, energy saving lamp, PC power supply unit), which represent a non-linear load were tested. Different variables were thoroughly tested for both presented algorithms: filter length, forgetting factor λ for QR-RLS and filter length, convergence constant μ for NLMS. The results were evaluated based on total harmonic distortion (THD), signal-to-noise ratio (SNR) root mean square error (RMSE) and percentage root mean square difference (PRD). The contribution of the article is to verify the functionality of NLMS and QR-RLS algorithms, especially the influence of individual parameters on successful harmonic compensation.**

Keywords - shunt active power filter (SAPF); total harmonic distortion (THD); normalized least mean squares (NLMS) algorithm; QR decomposition-based least squares (QR-RLS); non-linear loads.

I. INTRODUCTION

In recent years there is an intense increase in use of non-linear loads (variable speed drives, arc units, LED lighting systems and other non-linear loads), which causes an increase of harmonics in the power grid. The presence of harmonics causes several negative effects (e.g. heat loss in transformers, motors and transmission systems). Nowadays, two types of power filters are commonly used: passive [1] and active [2], [3]. Passive power filters (PFF) are inexpensive and achieve high efficiency. But PFF have following disadvantages: resonance; require more space; in the case of modifications in the system architecture, the original design becomes unusable and each specific harmonic requires one new PFF.

Active power filters (APF) can be classified as series active power filters, shunt active power filters (SAPF), or a combination of these types. APF simultaneously compensate harmonics and reactive current. Another advantage of APF is that it does not resonate and is able to work with a time-varying loads. The disadvantage of the APF is its higher switching loss compared to the passive filter. Important part of SAPF is control, which is provided by control algorithms. Algorithms can be divided into algorithms working in time domain [4], [5] and frequency domain [6], [7]. The control algorithms can be used for single-phase [8]–[10] and three-phase [11]–[14] system.

Our team focused on a development of a controlled adaptive modular inverter and dealt with the implementation of NLMS and QR-RLS algorithms in previous research [15]–[18]. The main goal is to determine the behavior of adaptive algorithms on rapidly changing dynamic processes before their deployment on adaptive modular inverter.

II. SHUNT ACTIVE POWER FILTER

SAPF is specially controlled voltage or current inverter that contains a very powerful computing unit. Computing unit is able to react to presence of harmonics and immediately compensate these harmonics and reactive power in the power grid. The function of SAPF is based on harmonic current compensation by injecting equal but inverse harmonic compensating current to point of common coupling (PCC). The quality of filtration depends on the control algorithm and the performance of the control unit, see [2], [11], [19]. Figure 1 shows block diagram of a SAPF.

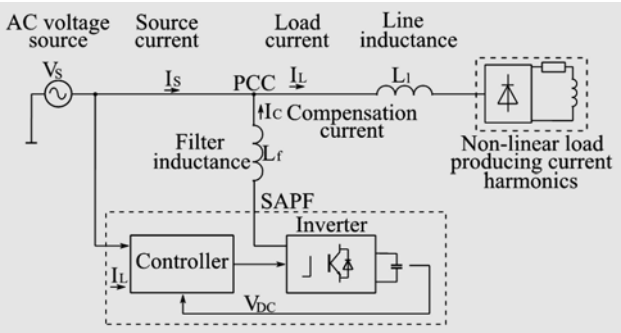

Figure 1. Block diagram of a shunt active power filter.

III. ADAPTIVE FILTRATION

Adaptive filter consists of linear FIR or IIR filter and an adaptive algorithm. Adaptive filters are used in an unknown environment, where pre identification is difficult or in a time-varying environment that cannot be predicted in the future.

Figure 2 shows general block diagram of FIR adaptive filter, where z^{-1} is a unit delay, $w_i(n)$ is the multiplicative gain, i is an integer with a value range of [0, n-1], *x(n)* is the reference signal, *d(n)* is the input signal, *e(n)* is the output error signal and *y(n)* is the output desired signal.

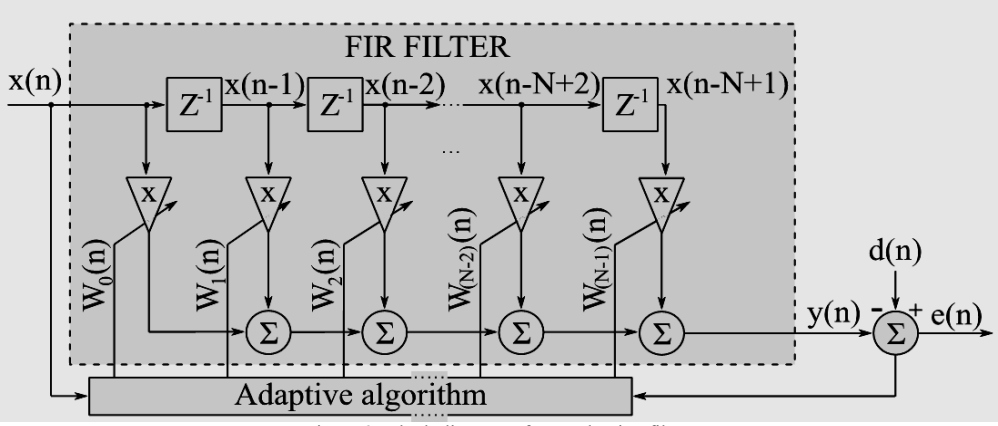

Figure 2. Block diagram of FIR adaptive filter.

The filter input signal is in the form of a column vector defined by the following equation:

$$\vec{x}(n) = \left[x(n)x(n-1)x(n-2)...x(n-N+1)\right]^T. \quad (1)$$

The filter coefficient vector is:

$$\vec{w}(n) = \left[w_0(n)w_1(n)w_2(n)...w_{N-1}(n)\right]^T. \quad (2)$$

The adaptive filter calculates the output signal y(n) by using the following equation:

$$y(n) = \vec{w}^T \vec{x}(n). \quad (3)$$

–A. Normalized Least Mean Squares Algorithm

The NLMS algorithm employs a variable step size for each iteration. This step size can improve the convergence speed of the adaptive filter [20], [21].

Each iteration of the NLMS algorithm requires three different steps, in this order:

- Filter output y(n) is calculated according to Equation (3).
- The value of the estimated error is calculated as e(n) = d(n) - y(n).
- The weights of the filter vector are updated by following equation:

$$\vec{w}(n+1) = \vec{w}(n) + \mu \cdot e(n) \frac{\vec{x}(n)}{\left\|\vec{x}(n)\right\|^2}, \quad (4)$$

where μ is the convergence constant or the step size of the NLMS algorithm.

–B. QR Decomposition-Based RLS

The QR-RLS uses the triangulation process and performs good mathematical properties. This is due to the robust QR decomposition [22], [23] that contains the Givens transformation. This algorithm guarantees positive definiteness and is numerically stable.

- Filter output y(n) is calculated according to Equation (3).
- The problem of estimating QR-RLS can be determined by equation (5), given an observation vector d(n) of size N, we want to estimate some reference signal x(n). The estimation error e(t) is calculated according to following equation:

$$e(n) = d(n) - \vec{w}^T(n)\vec{x}(n), \quad (5)$$

where $\vec{w}^T(n)$ is the weight vector of size N, $\vec{x}(n)$ is the input sample vector.

- The weights of the filter vector are updated by following equation:

$$\vec{w}(n) = R^{-1}(n)\vec{p}(n), \quad (6)$$

where p(n) is the corresponding vector and R(n) is triangular matrix.

More information about the QR-RLS are provided in [24]–[26], where algorithm is explained in detail.

IV. EXPERIMENTS

Figure 3 shows block diagram of the experiments, which were carried out with measured data. Voltage and current on one-phase load were measured using National Instruments data acquisition hardware. The voltage was measured by an NI 9225 voltage module and current was measured by an NI 9227 current module. Both NI 9225 and NI 9227 modules were inserted into a cDAQ 9185 chassis, which was connected to PC by Ethernet. Instantaneous values of voltage and current were measured using simultaneous sampling with sampling rate of 50k Samples/s per channel. Using FFT, we obtained amplitude of the fundamental harmonic, which serves as the reference sinus waveform.

The compensation current pattern, which is obtained by adaptive filter is sent to the inverter, where the compensating current is generated. The compensating current is injected to the PCC in the opposite phase. Since the experiments were performed in a simulation mode, instead of using the inverter, we implemented delay of 100 µs. The 100 µs delay was chosen because it is the expected delay value of our modular inverter. After injecting compensating current to the PCC, the current sinusoidal waveform in the electrical grid should occur. After filtration, the parameters THD, SNR, RMSE and PRD are computed. The measured current of one-phase load was read from the file as if they were plugged into the socket. Voltage values were not used as the feedback effect cannot be investigated without the inverter.

Figure 4 shows one-phase waveform of the current with a substantial distortion of five nonlinear loads, while each load has a time window length of 100ms. These loads immediately changed to investigate the effect of rapid load changes on the adaptive filter. FFT and THD for each load are on fig. 5 to fig. 9.

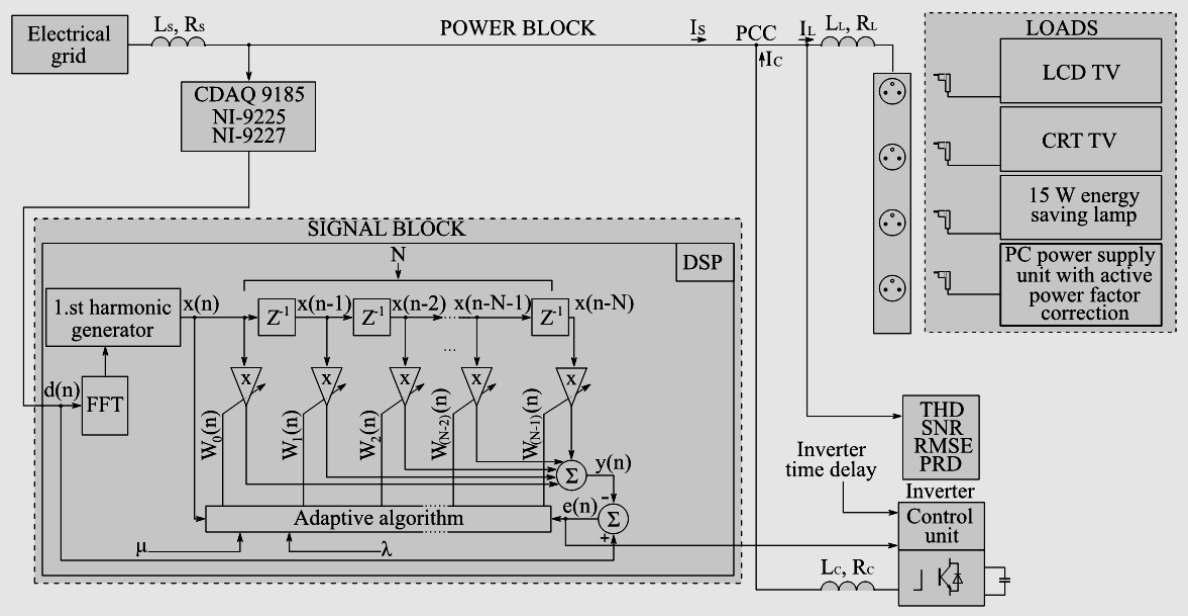

Figure 3. Block diagram of the experiment.

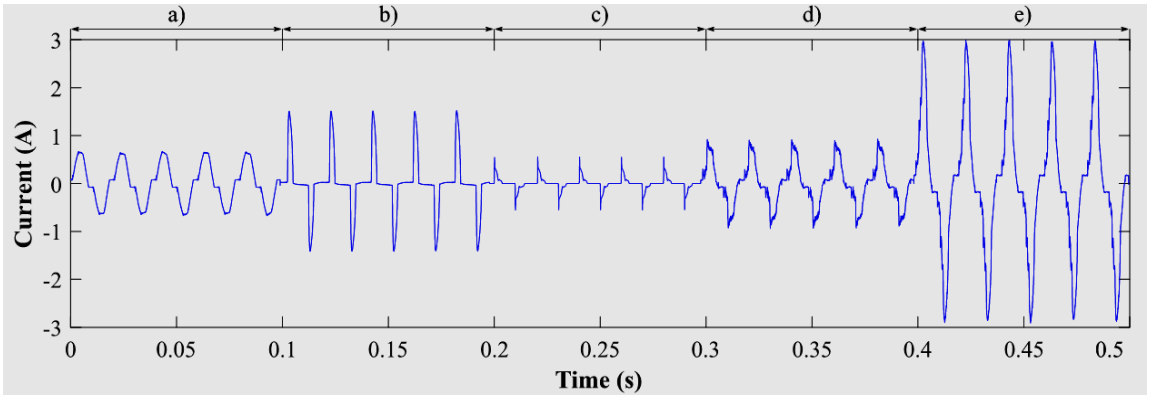

Figure 4. The waveforms of the individual tested loads a) LCD TV b) CRT TV c) 15 W energy saving lamp d) PC power supply unit with active power factor correction e) all loads connected at once.

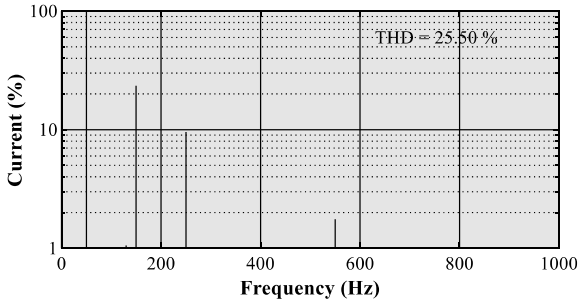

Figure 5. FFT of LCD TV.

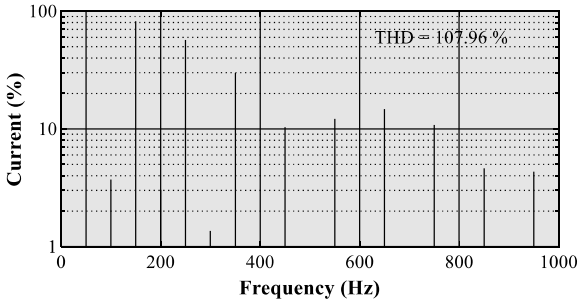

Figure 6. FFT of CRT TV.

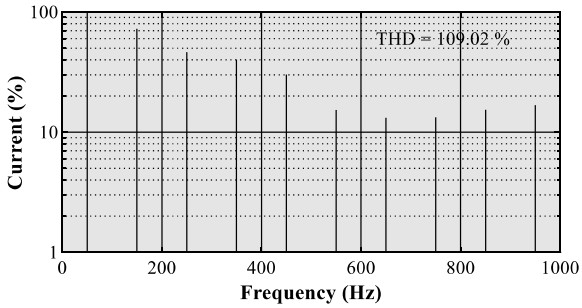

Figure 7. FFT of 15 W energy saving lamp.

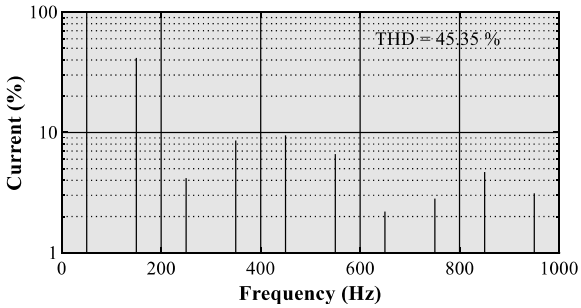

Figure 8. FFT of PC power supply unit with active power factor correction.

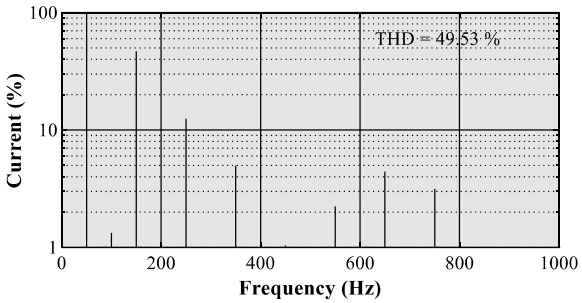

Figure 9. FFT of all loads connected at once.

V. RESULTS

Due to the inverter delay that was added in the simulations, the current does not have a purely sinusoidal waveform after the compensation. However, from the perspective of higher harmonic filtration, this is still a significant improvement. Figures 10 and 11 show the waveform of the reference (green) and input (red) signals after filtration.

It is noticeable from Fig. 10 and 11 that the NLMS algorithm has a convergence time of approximately 60 ms and the QR-RLS algorithm has a convergence time below 10 ms. The value of convergence time varies according to the adaptive filter setting, especially in case of NLMS algorithm.

Figure 12 shows FFT waveforms before and after application of adaptive algorithms NLMS and QR-RLS. It is visible from these FFTs that higher harmonics have been suppressed.

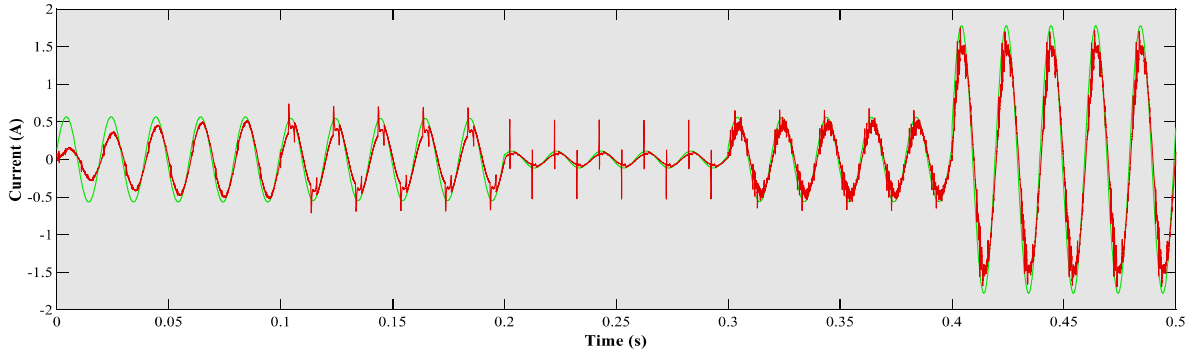

-Figure 10. Input signal after filtration using NLMS algorithm; filter length 70, step size 0.001, time delay 100 µs.

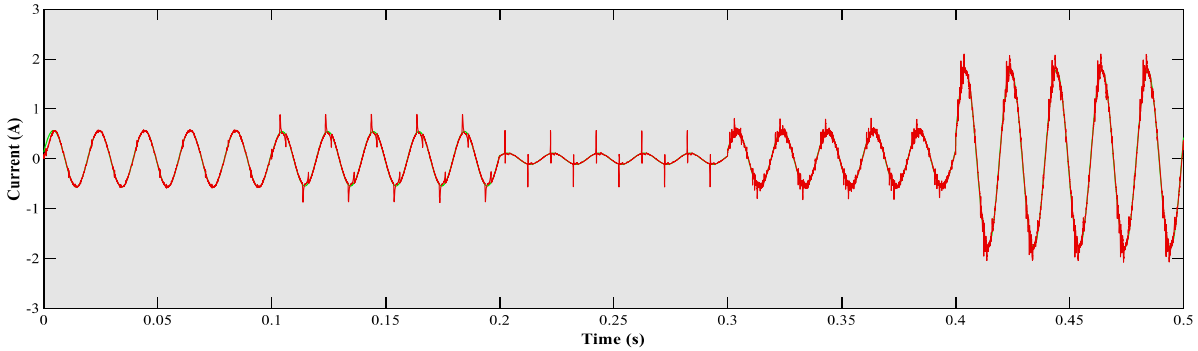

-Figure 11. Input signal after filtration using QR-RLS algorithm; filter length 2, forgetting factor 1, time delay 100 µs.

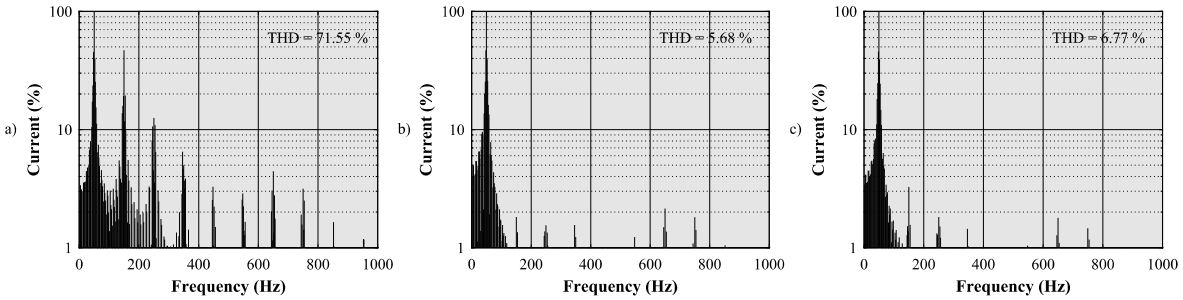

-Figure 12. FFT of input signal in length 0-500 ms a) before filtration, b) after applying NLMS algorithm; filter length 70, step size 0.001, time delay 100 µs c) after applying QR-RLS algorithm; filter length 2, forgetting factor 1, time delay 100 µs.

TABLE I. RESULTS OF THE EXPERIMENT USING ADAPTIVE ALGORITHM NLMS.

NLMS	**Filter Length (-) = 50**				**Filter Length (-) = 70**			
µ (-)	THD (%)	SNR_{OUT} (dB)	$RMSE_{OUT}$ (A)	PRD_{OUT} (%)	THD (%)	SNR_{OUT} (dB)	$RMSE_{OUT}$ (A)	PRD_{OUT} (%)
0.0005	7.85	10.48	0.0012	29.94	7.66	10.69	0.0012	29.21
0.001	6.02	11.11	0.0011	27.82	5.68	11.55	0.0011	26.47
0.005	21.46	11.34	0.0011	27.11	19.61	12.22	0.0010	24.48

-TABLE II. RESULTS OF THE EXPERIMENT USING ADAPTIVE ALGORITHM QR-RLS.

QR-RLS	**Filter Length (-) = 2**				**Filter Length (-) =20**			
λ (-)	THD (%)	SNR_{OUT} (dB)	$RMSE_{OUT}$ (A)	PRD_{OUT} (%)	THD (%)	SNR_{OUT} (dB)	$RMSE_{OUT}$ (A)	PRD_{OUT} (%)
0.99	57.07	7.43	0.0017	42.50	Unstable	Unstable	Unstable	Unstable
0.999	4.19	19.92	0.00041	10.10	5.65	16.95	0.00058	14.20
0.9999	6.31	20.30	0.00039	9.66	6.20	19.95	0.00041	10.06
1	6.77	20.16	0.00040	9.81	6.66	20.08	0.00040	9.90

Filtration quality can be evaluated based on the parameters THD, RMSE, and PRD, where the values should be as low as possible and the parameter SNR, where the value should be as high as possible.

From table 1, it can be seen that the best adaptive filter setting is at filter length 70 and step size 0.001. At this setting, the lowest THD is achieved and with decreasing step size convergence time rises.

From table 2, the results indicate that it is not advisable to set the forgetting factor below 0.999, as there is deterioration in the power quality or an unstable behavior of the adaptive filter. The best result was achieved by setting the forgetting factor 0.999 and filter length 2.

VI. CONCLUSION

The experiments were based on simulated adaptive testing platform for NLMS and QR-RLS SAPF control algorithms. A delay of the controlled adaptive modular inverter was added to the simulation. The experiments focused on the quality of harmonic suppression from the power grid. Harmonic suppression is needed where non-linear loads are widely used.

The experiments were performed on real data that were measured on consumer electronics. The adaptive system was investigated for NLMS and QRLS algorithms at various settings. Experiments have shown that the setting of the adaptive system has a significant influence on the filtration quality. The results of the experiments were evaluated based on THD, SNR, RMSE and PRD.

The results show that the adaptive harmonic suppression system is very effective. Both NLMS and QR-RLS algorithms achieve very similar THD values, but NLMS algorithm has a lower convergence speed and larger steady state error than RLS algorithm, which is more computationally complicated. Therefore, the NLMS algorithm appears to be a more appropriate option for DSP implementation.

ACKNOWLEDGMENT

This article was supported by the Ministry of Education of the Czech Republic (Project No. SP2019/85 and SP2019/118). This work was supported by the European Regional Development Fund in the Research Centre of Advanced Mechatronic Systems project, project number CZ.02.1.01/0.0/0.0/16 019/0000867 within the Operational Programme Research, Development and Education. This work was supported by the European Regional Development Fund in A Research Platform focused on Industry 4.0 and Robotics in Ostrava project, CZ.02.1.01/0.0/0.0/17 049/0008425 within the Operational rogramme Research, Development and Education.

REFERENCES

[1] M.-H. Chen, "Development of Shunt-Type Three-Phase Active Power Filter with Novel Adaptive Control for Wind Generators," *Sci. World J.*, vol. 2015, pp. 1–10, 2015.

[2] M. Diab, M. El-Habrouk, T. H. Abdelhamid, and S. Deghedie, "Survey of Active Power Filters Configurations," In *2018 IEEE International Conference on System, Computation, Automation and Networking (ICSCA)*, Pondicherry, 2018, pp. 1–14.

[3] B. Singh, K. Al-Haddad, and A. Chandra, "A review of active filters for power quality improvement," *IEEE Trans. Ind. Electron.*, vol. 46, no. 5, pp. 960–971, Oct. 1999.

[4] R. S. Herrera, P. Salmeron, and H. Kim, "Instantaneous Reactive Power Theory Applied to Active Power Filter Compensation: Different Approaches, Assessment, and Experimental Results," *IEEE Trans. Ind. Electron.*, vol. 55, no. 1, pp. 184–196, Jan. 2008.

[5] L. Asiminoael, F. Blaabjerg, and S. Hansen, "Detection is key - Harmonic detection methods for active power filter applications," *IEEE Ind. Appl. Mag.*, vol. 13, no. 4, pp. 22–33, Jul. 2007.

[6] S. Rechka, E. Ngandui, J. Xu, and P. Sicard, "Performance evaluation of harmonics detection methods applied to harmonics compensation in presence of common power quality problems," *Math. Comput. Simul.*, vol. 63, no. 3–5, pp. 363–375, Nov. 2003.

[7] A. Pigazo, V. M. Moreno, and E. J. Estebanez, "A Recursive Park Transformation to Improve the Performance of Synchronous Reference Frame Controllers in Shunt Active Power Filters," *IEEE Trans. Power Electron.*, vol. 24, no. 9, pp. 2065–2075, Sep. 2009.

[8] M. T. Haque, "Single-phase PQ theory," In *2002 IEEE 33rd Annual IEEE Power Electronics Specialists Conference. Proceedings (Cat. No.02CH37289)*, Cairns, Qld., Australia, 2002, vol. 4, pp. 1815–1819.

[9] S. A. Oliveira da Silva, R. Novochadlo, and R. A. Modesto, "Single-phase PLL structure using modified p-q theory for utility connected systems," In *2008 IEEE Power Electronics Specialists Conference*, Rhodes, Greece, 2008, pp. 4706–4711.

[10] V. Khadkikar and A. Chandra, "Control of single-phase UPQC in synchronous d-q reference frame," In *2012 IEEE 15th International Conference on Harmonics and Quality of Power*, Hong Kong, China, 2012, pp. 378–383.

[11] Q.-N. Trinh and H.-H. Lee, "An Advanced Current Control Strategy for Three-Phase Shunt Active Power Filters," *IEEE Trans. Ind. Electron.*, vol. 60, no. 12, pp. 5400–5410, Dec. 2013.

[12] M. Aredes and E. H. Watanabe, "New control algorithms for series and shunt three-phase four-wire active power filters," *IEEE Trans. Power Deliv.*, vol. 10, no. 3, pp. 1649–1656, Jul. 1995.

[13] M. Aredes, J. Hafner, and K. Heumann, "Three-phase four-wire shunt active filter control strategies," *IEEE Trans. Power Electron.*, vol. 12, no. 2, pp. 311–318, Mar. 1997.

[14] M. I. M. Montero, E. R. Cadaval, and F. B. Gonzalez, "Comparison of Control Strategies for Shunt Active Power Filters in Three-Phase Four-Wire Systems," *IEEE Trans. Power Electron.*, vol. 22, no. 1, pp. 229–236, Jan. 2007.

[15] R. Martinek, J. Vanus, and P. Bilik, "New Strategies for Application of Recursive Least Square Algorithm in Active Power Filters," In *8th International Scientific Symposium on Electrical Power Engineering (Elektroenergetika), Stara Lesna, Slovakia*, 2015, pp. 344–347.

[16] R. Martinek, J. Vanus, M. Kelnar, and P. Bilik, "Control methods of active power filters using soft computing techniques," In *8th International scientific symposium on electrical power engineering (Elektroenergetika), Stara Lesna, Slovakia*, 2015, pp. 363–366.

[17] R. Martinek, J. Vanus, P. Bilik, T. Stratil, and J. Zidek, "An Efficient Control Method of Shunt Active Power Filter Using ADALINE," *IFAC-Pap.*, vol. 49, no. 25, pp. 352–357, 2016.

[18] R. Martinek, J. Rzidky, R. Jaros, P. Bilik, and M. Ladrova, "Least Mean Squares and Recursive Least Squares Algorithms for Total Harmonic Distortion Reduction Using Shunt Active Power Filter Control," *Energies*, vol. 12, no. 8, p. 1545, Apr. 2019.

[19] D. A. Tamboli and R. H. Chile, "Reference signal generation for shunt active power filter using adaptive filtering approach," In *2015 International Conference on Industrial Instrumentation and Control (ICIC)*, Pune, India, 2015, pp. 766–770.

[20] D. L. Duttweiler, "Proportionate normalized least-mean-squares adaptation in echo cancelers," *IEEE Trans. Speech Audio Process.*, vol. 8, no. 5, pp. 508–518, Sep. 2000.

[21] S. C. Douglas, "A family of normalized LMS algorithms," *IEEE Signal Process. Lett.*, vol. 1, no. 3, pp. 49–51, Mar. 1994.

[22] V. Gopalakrishna and P. Khanikar, "Adaptation Behavior of Pipelined Adaptive Digital Filters," 2004.

[23] C. K. Singh, S. H. Prasad, and P. T. Balsara, "VLSI Architecture for Matrix Inversion using Modified Gram-Schmidt based QR Decomposition.," In *VLSI Design*, 2007, pp. 836–841.

[24] K. J. Raghunath and K. K. Parhi, "Finite-precision error analysis of QRD-RLS and STAR-RLS adaptive filters," *IEEE Trans. Signal Process.*, vol. 45, no. 5, pp. 1193–1209, May 1997.

[25] J. Ma, E. F. Deprettere, and K. K. Parhi, "Pipelined Cordic based QRD-RLS adaptive filtering using matrix lookahead," In *1997 IEEE Workshop on Signal Processing Systems. SiPS 97 Design and Implementation formerly VLSI Signal Processing*, Leicester, UK, 1997, pp. 131–140.

[26] L. Gao and K. K. Parhi, "Hierarchical pipelining and folding of QRD-RLS adaptive filters and its application to digital beamforming," *IEEE Trans. Circuits Syst. II Analog Digit. Signal Process.*, vol. 47, no. 12, pp. 1503–1519, Dec. 2000.